Nuclear Instruments and Methods in Physics Research B 398 (2017) 35–41

Contents lists available at ScienceDirect

Nuclear Instruments and Methods in Physics Research B

journal homepage: www.elsevier.com/locate/nimb

GaAs radiovoltaic cell enhanced by Y_2SiO_5 crystal for the development of new gamma microbatteries

Zheng-Rong Zhang [a], Xiao-Bin Tang [a,b,*], Yun-Peng Liu [a,b], Zhi-Heng Xu [a], Zi-Cheng Yuan [a], Kai Liu [a], Wang Chen [a]

[a] Department of Nuclear Science and Engineering, Nanjing University of Aeronautics and Astronautics, 29 General Road, Jiangning District, Nanjing 211106, China
[b] Jiangsu Key Laboratory of Material and Technology for Energy Conversion, Nanjing 211106, China

ARTICLE INFO

Article history:
Received 28 November 2016
Received in revised form 8 March 2017
Accepted 11 March 2017

Keywords:
GaAs photovoltaic material
Radiovoltaic cell
Y_2SiO_5 crystal
Multi-level structure
Microbattery

ABSTRACT

The design of a new gamma/GaAs multi-level structure radiovoltaic microbattery enhanced by an Y_2SiO_5 (YSO) crystal is proposed. By introducing the YSO crystal in the GaAs radiovoltaic cell, the output power from the cell was significantly improved. We focus on the enhancement mechanisms of performance output in one level of a multi-level structure. The radioluminescence spectra of the YSO crystal revealed its fluorescence in the wavelength range of approximately 300–700 nm. Light at the exact wavelength would normally be totally absorbed by the GaAs photovoltaic material. The radiovoltaic cells were tested using an X-ray tube to simulate the gamma rays emitted by a gamma-radioactive source. Experimental investigation showed that the YSO crystal can increase the cell output power. The output power of the new GaAs/YSO radiovoltaic cell was enhanced by more than four times compared to that of the conventional GaAs radiovoltaic cell. In addition, considering the importance of the YSO crystal in the new GaAs/YSO radiovoltaic cell, the irradiation resistance of the YSO crystal under X-ray excitation was also analysed.

1. Introduction

With the rapid development of micro-electromechanical systems (MEMS) in military, aerospace and biomedical applications, there is an increasing demand for power sources [1–4]. A promising candidate is the radiovoltaic battery for use as a power supply in MEMS because of its high energy density, stability and long life [5–8]; however, a rapid degradation in both alpha- and betavoltaic microbatteries (the main representatives of the class known as radiovoltaic batteries) was observed because of the energetic charged particles that induced defects therein [9–12]. Low-energy charged particles (such as α and β particles) can minimize radiation damage in the semiconductor, but are easily absorbed by radioisotopes themselves when low-energy sources are used in microbatteries; this eventually leads to a very low conversion efficiency [13,14]. However, an alternative radioactive isotope that would avoid these problems is a γ source that can reduce device damage risks, resulting in a substantially increased microbattery lifetime. Therefore, a γ source can be used as the excitation source for such a microbattery. X-ray emitters can also be used for the development of long-life microbatteries, with reduced damage risk for the converter device. A prototype GaAs ^{55}Fe radioisotope microbattery was developed using a low-energy ^{55}Fe radioisotope X-ray source and a GaAs device [10,11].

Because γ photons could pass through a single GaAs device, more than one GaAs device needs to be used as the semiconductor material in a GaAs γ-ray microbattery (Fig. 1) to improve the γ-ray energy utilisation. In this situation, most of the γ-ray energy is absorbed by the GaAs substrate and the back electrode, and less energy is absorbed by the GaAs photovoltaic (PV) material; this is because the thickness of the PV material is much less than those of the GaAs substrate and the back electrode, thus leading to a continuous low performance. To exploit the γ-ray energy to a greater extent, this paper proposes the introduction of the Y_2SiO_5 (YSO) crystal for a multi-layer structured GaAs γ-ray microbattery. Fig. 2 shows the structure of the new multi-level gamma/GaAs radiovoltaic microbattery. A piece of the YSO crystal and the GaAs device were considered as one level in the new multi-level gamma/GaAs radiovoltaic microbattery. The theoretical schematic of the new gamma/GaAs radiovoltaic microbattery (indicated by the dotted box in Fig. 2) is shown in Fig. 3.

As illustrated in Fig. 3, the new gamma/GaAs radiovoltaic microbattery is composed of three parts: a γ source, a GaAs device (the back electrode/substrate/GaAs PV material) and the YSO crystal.

* Corresponding author at: Department of Nuclear Science and Engineering, Nanjing University of Aeronautics and Astronautics, Nanjing, China.
E-mail address: tangxiaobin@nuaa.edu.cn (X.-B. Tang).

http://dx.doi.org/10.1016/j.nimb.2017.03.060
0168-583X/

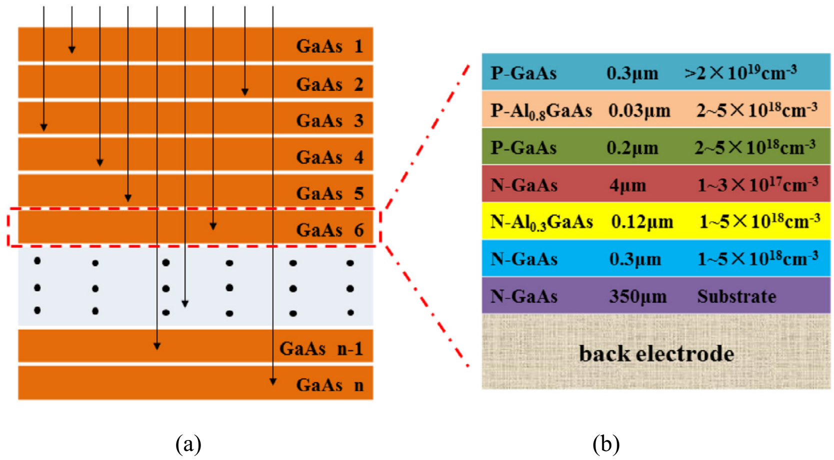

Fig. 1. Structure of (a) multi-level GaAs γ-ray microbattery and (b) the GaAs device

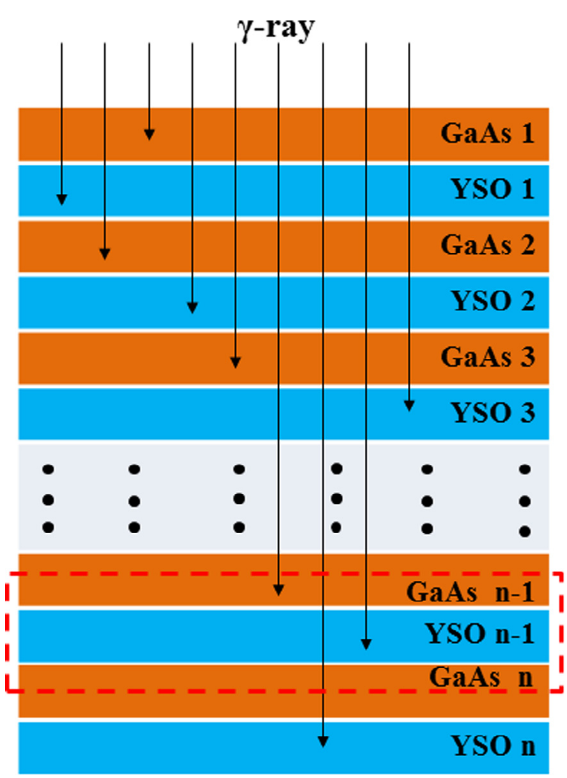

Fig. 2. Structure of the new multi-level gamma/GaAs radiovoltaic microbattery.

The working principle of the new gamma/GaAs radiovoltaic microbattery is as follows: when γ photons pass through the back electrode into the PV material, many electron–hole pairs are generated. The γ photons then penetrate the PV material and move towards the YSO crystal and produce luminescence. The PV material receives radioluminescence from the YSO crystal and creates many electron–hole pairs. All these electron–hole pairs are separated by the built-in electrical field, and the battery delivers an output current after being connected to an external circuit.

This paper focuses on discussing the mechanisms designed to enhance microbattery output performance in one level of a multi-level structure. In the experiment, the tunable X-ray emissions from the X-ray tube were used to simulate the γ-rays emitted by a γ-radioactive source because of the modulation of the intensity of the emitted X-rays [15,16]. The findings indicate that an YSO crystal can absorb the γ-rays that penetrate the GaAs device, thus generating radioluminescence. The radioluminescence can increase the output power of the battery to a significant extent. We also studied the irradiation resistance of the YSO crystal. The results of this research indicate that such a cell is stable and efficient over long periods of time.

2. Materials and methods

2.1. Experimental materials

An X-ray tube (Shanghai KeyWay Electron Company Ltd. KYW900A, China) was used to simulate the γ-rays in one level of the multi-level structured gamma/GaAs radiovoltaic microbattery. The specific parameter values of the X-ray tube are listed in Table 1.

An equivalent model was built to represent the relationship between the X-ray and γ-ray energy spectra by GEANT4 when the tube voltage was 60 kV. The X-ray energy spectrum was obtained by GEANT4 as shown in Fig. 4: it can be observed that the energy thereof is mainly concentrated in the low-energy section. The horizontal and vertical coordinates represent the electron energy and the photon numbers generated by an electron at different energies, respectively.

The number of X-ray photons (A) generated by the X-ray tube per second can be calculated by Eq. (1) as follows:

$$A = \frac{IT}{e} \times n_p \tag{1}$$

where I is the tube current, $e = 1.602 \times 10^{-19}$ C is the charge of the electron, $T = 1$ s is the time and $n_p = 0.001157$ is the number of protons generated by an electron at the tube voltage of 60 kV. The activities of the gamma sources were calculated to be 5.77×10^{12} and 7.22×10^{12} Bq for the tube currents of 800 and 1000 μA, respectively; the average energy of X-rays was 16.73 keV at tube voltages of up to 60 keV.

A GaAs device was used as the converter material: this offers several advantages over a conventional silicon device such as its compact structure [17], direct band gap structures, large light-absorption coefficient, wide band gap [18,19], low leakage currents [20,21] and high radiation resistance [22]. The thickness of the GaAs device was less than 2 mm, and the active area measured 10 mm × 10 mm. The GaAs device is illustrated in Fig. 5, and its specific parameter values are listed in Table 2.

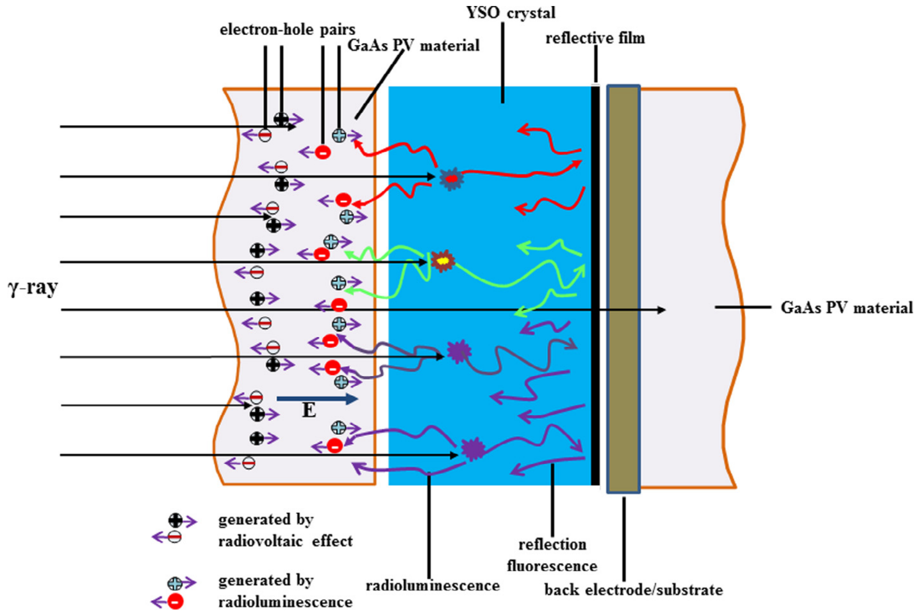

Fig. 3. Schematic of the new gamma/GaAs radiovoltaic microbattery.

Table 1
Key parameters of the X-ray tube.

Anode voltage	Anode current	Maximum power	Filament voltage	Filament current
60 kV	0–1 mA	60 W	2.5 V	60 kV/1 mA, I_f = 1.7 A
Thickness of the beryllium window	Target angle	Focus spot size	Grounded mode	Target
200 μm	10°	0.1 mm × 0.1 mm	Grounded-cathode	Tungsten

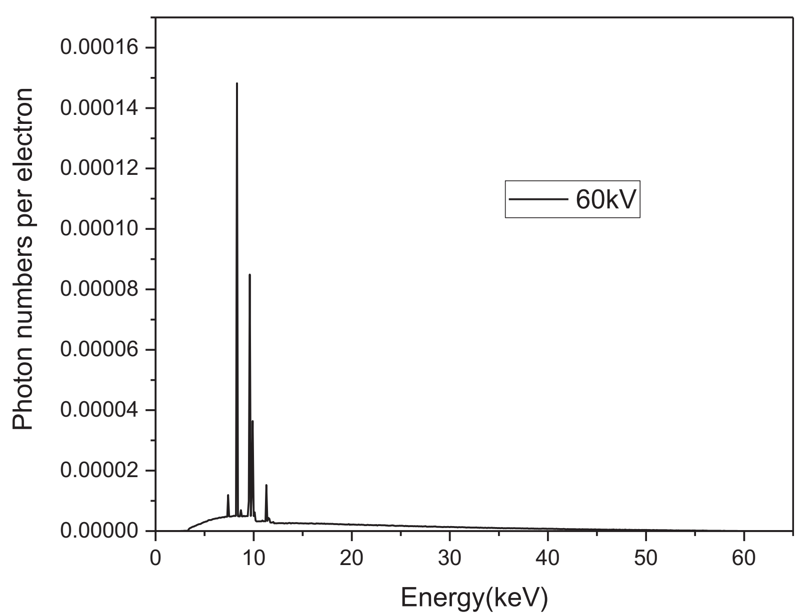

Fig. 4. X-ray energy spectrum for a tube voltage of 60 kV.

YSO crystals were used as luminescent materials in the experiment, as shown in Fig. 6. By using an ultraviolet–visible spectrophotometer (Shimadzu UV-2550, Japan), the transmission spectra and the absorption spectra (Fig. 7) of the YSO crystal were measured over the scanning range from 400 to 800 nm. The values of various parameters of the YSO crystal, such as its size, mass and optical spectrum, are listed in Table 3.

The YSO crystal has a monoclinic crystal structure [23] and is an excellent optical material [24–26]. It has a high luminous efficiency, excellent resistance to chemical corrosion and good heat stability [27–30]; therefore, it has a great potential for broader application. Table 3 shows that the average transmission rate of the YSO crystal in the visible range is above 93%. This high transmission rate indicates that the radioluminescence released from

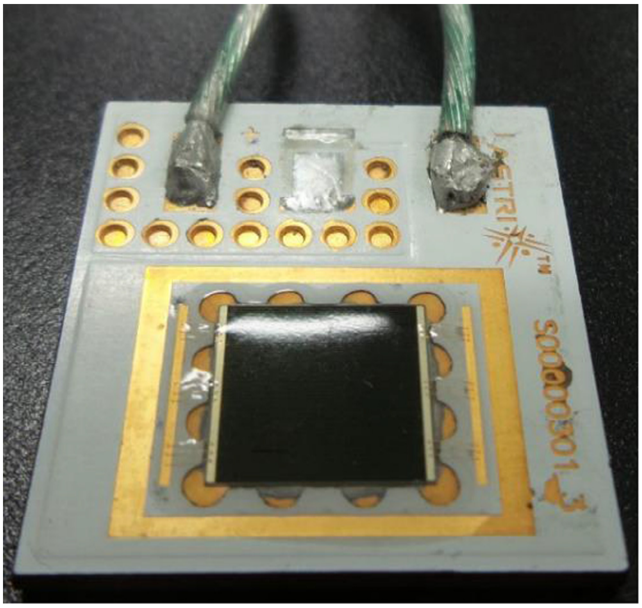

Fig. 5. The picture of the GaAs device.

the YSO crystal is not easily absorbed by the crystal itself, thus resulting in a high transmission efficiency.

2.2. Experimental measurements

2.2.1. Radioluminescence spectra of the YSO crystal and spectral responsivity of the GaAs device

With the chosen KYW900A X-ray tube (tube voltage: 30 kV, tube current: 600 μA) excitation, the radioluminescence spectra of the YSO crystal under test were measured by using a Cary Eclipse fluorescence spectrophotometer (Agilent Technologies G9800a, Malaysia), and the spectral response curve of the GaAs device was measured by quantum efficiency spectrometer (Bentham PVE300, Britain).

2.2.2. I–V test

The electrical properties of the microbatteries, such as their short circuit current (I_{sc}) and open circuit voltage (V_{oc}), were measured at room temperature by using a dual-channel system sourcemeter instrument (Keithley 2636A, USA). The maximum output power (P_{max}), fill factor (*FF*) and experimental microbattery efficiency (η) were calculated as follows:

$$P_{max} = V_{max} \times I_{max} \tag{2}$$

$$FF = \frac{V_{max} \times I_{max}}{V_{oc} \times I_{sc}} \tag{3}$$

$$\eta = \frac{V_{oc} \times I_{sc} \times FF}{P_{in}} \times 100\% \tag{4}$$

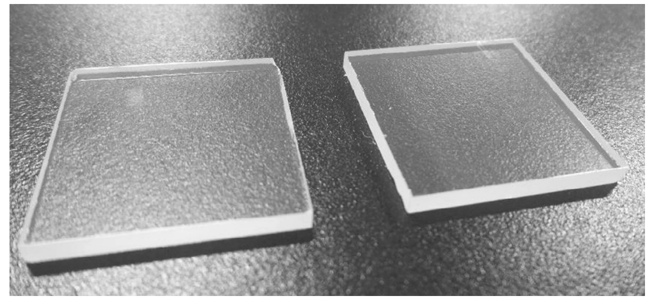

Fig. 6. Picture of the Y_2SiO_5 crystal.

where P_{max} is the maximum output power of the battery; V_{max} and I_{max} are the voltage and the current, respectively, at the maximum power point; and P_{in} is the incident X-ray power, which was obtained from the integral of the X-ray energy spectrum.

3. Results and discussion

3.1. Optical performances of the YSO crystal

The radioluminescence spectra of the YSO crystal are shown in Fig. 8. Fig. 9 shows the relationship between the external quantum efficiency of the GaAs device and the incident wavelength.

From Fig. 8, it can be observed that the maximum wavelength was approximately 420 nm, and the FWHM was approximately 78 nm. There was a good match between the radioluminescence spectra of the YSO crystal and the spectral response curves of the GaAs device; thus, radioluminescence that penetrates the PV material at that exact wavelength would normally be absorbed efficiently without waste.

3.2. Electrical performances of the microbattery

As the γ rays have strong penetrability and can pass through a GaAs device easily, the design of the new gamma/GaAs multi-level structured radiovoltaic microbattery (Fig. 2) is proposed to improve the γ-ray energy utilisation.

Considering the γ-ray energy utilisation and the performance output of this microbattery, the advantages and shortcomings of two different battery structures were analysed. Two different battery structures (Model A: "X-ray + back electrode/substrate/GaAs PV material" and Model B: "X-ray + back electrode/substrate/GaAs PV material + YSO crystal") were tested. Model A was deemed the more "conventional structure" and Model B the "YSO crystal-enhanced structure". The aim of this project is to discuss whether the YSO crystal offers any enhancement of the performance of the cell under X-ray excitation. The tube voltage was set to 60 kV, and the tube current was set to 800 and 1000 μA, corresponding to the two different X-ray excitation conditions.

The structure schematic and the prototype of the two kinds of battery are shown in Fig. 10. The actual size of the cell was

Table 2
Parameters of the GaAs device.

Layer no.	Material	Composition(x)	Thickness(nm)	Doping level(cm^{-3})	Type
6	GaAs	–	300	>2×10^{19}	P
5	$Al_{(x)}GaAs$	0.8	30	2–5×10^{18}	P
4	GaAs	–	200	2–5×10^{18}	P
3	GaAs	–	4000	1–3×10^{17}	N
2	$Al_{(x)}GaAs$	0.3	120	1–5×10^{18}	N
1	GaAs	–	300	1–5×10^{18}	N
Substrate	GaAs	–	350,000	1–4×10^{18}	N

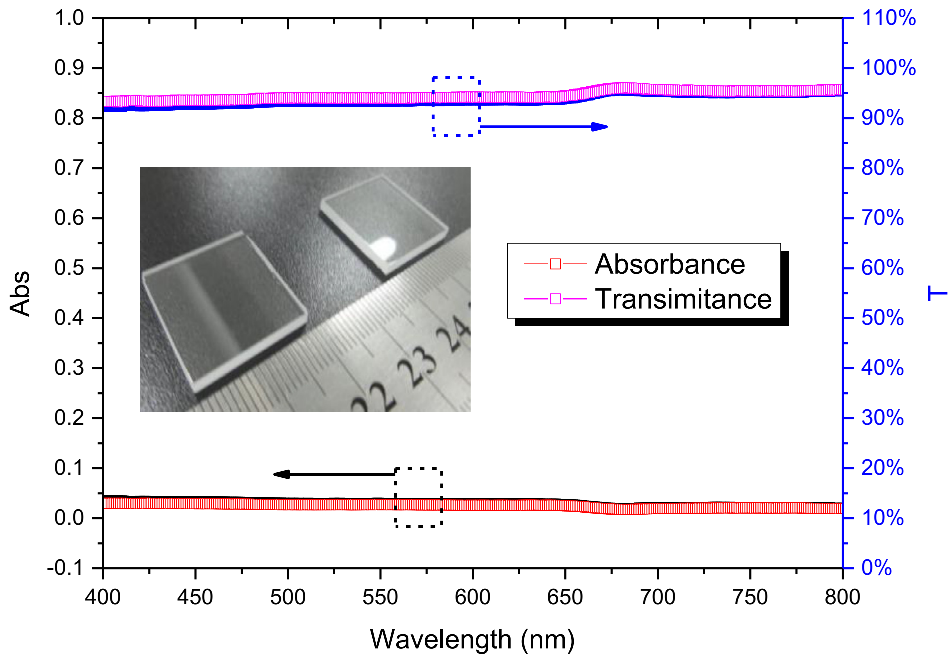

Fig. 7. Transmission spectra and absorption spectra of the Y_2SiO_5 crystal.

Table 3
Key parameters of the YSO crystal.

Dimensions (mm)	Mass (g)	*T*	Abs
20 × 20 × 2	3.600	>93%	~0.03

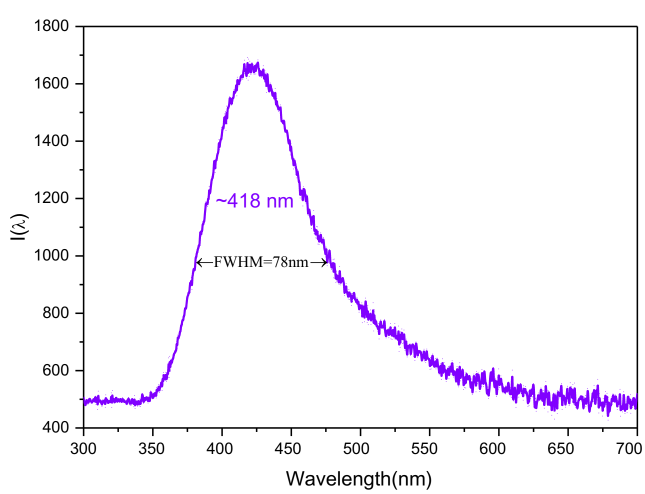

Fig. 8. Radioluminescence spectra of the YSO crystal under X-ray excitation.

10 mm × 10 mm. The *I–V* characteristics were measured during the continuous, direct X-ray exposure. *I–V* curves of the two battery structures are shown in Fig. 11. The maximum output power comparison chart for the two battery structures was obtained by calculation, as shown in Fig. 12.

As shown in Figs. 11 and 12, I_{sc}, V_{oc} and P_{max} of the YSO crystal-enhanced structure were far greater than those of the conventional structure under the same excitation conditions.

A comparative analysis of the electrical parameters of Models A and B is given in Table 4. It can be observed that at tube voltages of up to 60 keV, the short-circuit currents of the YSO crystal-enhanced structure were 2.65 and 2.77 times greater than those of the conventional structure for the tube currents of 800 and 1000 μA, respectively. Moreover, the values of P_{max} of the YSO crystal-enhanced structure were 4.08 and 4.37 times greater than those of the conventional structure for the tube currents of 800 and 1000 μA, respectively. This result indicates that the YSO crystal can significantly improve the output power of the cell.

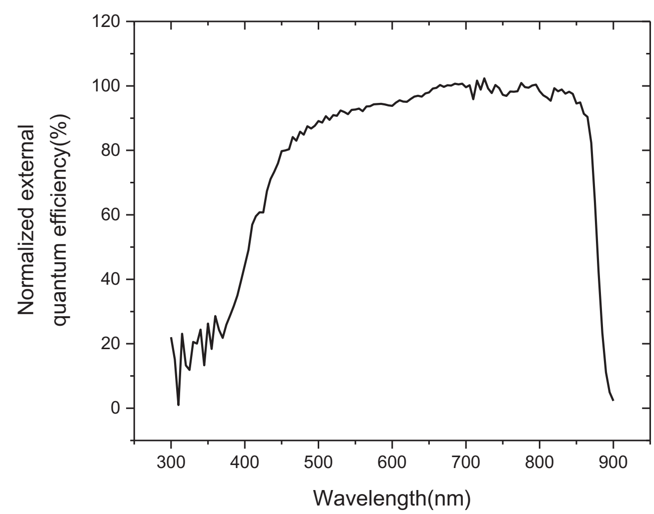

Fig. 9. Spectral response curves of the GaAs device.

3.3. Influences of irradiation on the YSO crystal

An experimental study of the effects of irradiation on the YSO crystal was carried out depending on the structure: X-ray + YSO + GaAs device, and the excitation conditions were as follows: (1) tube voltage: 17 kV, tube current: 400 μA; (2) tube voltage: 17 kV, tube current: 800 μA; (3) tube voltage: 52 kV, tube current:

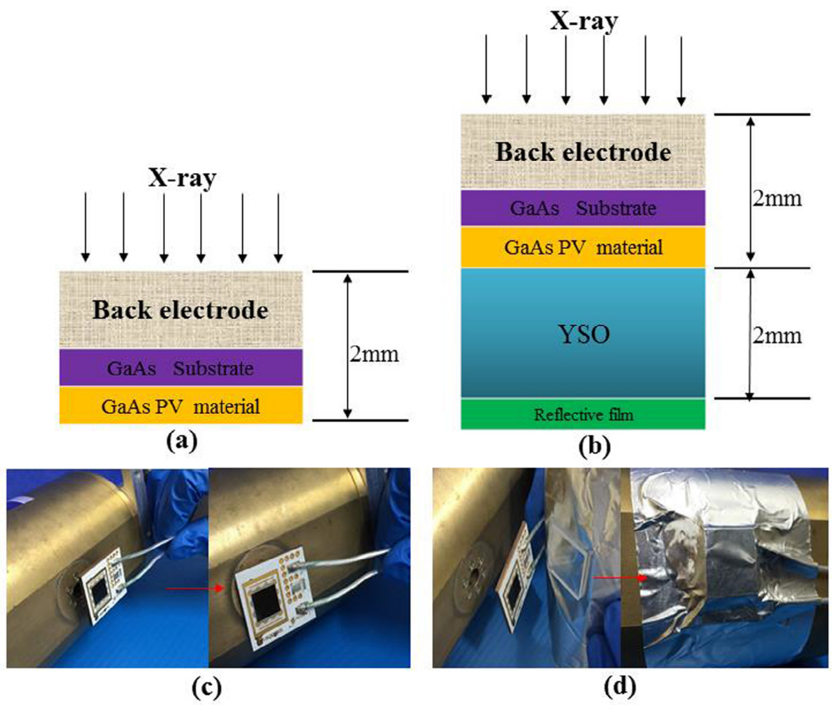

Fig. 10. (a) Schematic of the conventional structure, (b) schematic of the YSO-enhanced structure, (c) prototype of the conventional structure and (d) prototype of the YSO crystal-enhanced structure.

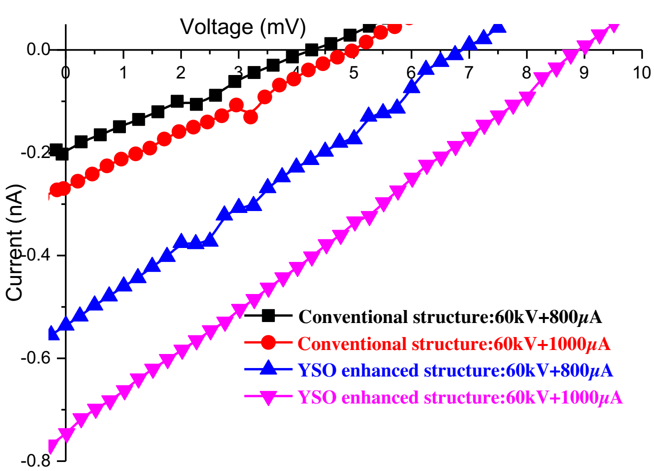

Fig. 11. *I*–*V* curves of the two battery structures under different X-ray excitation conditions.

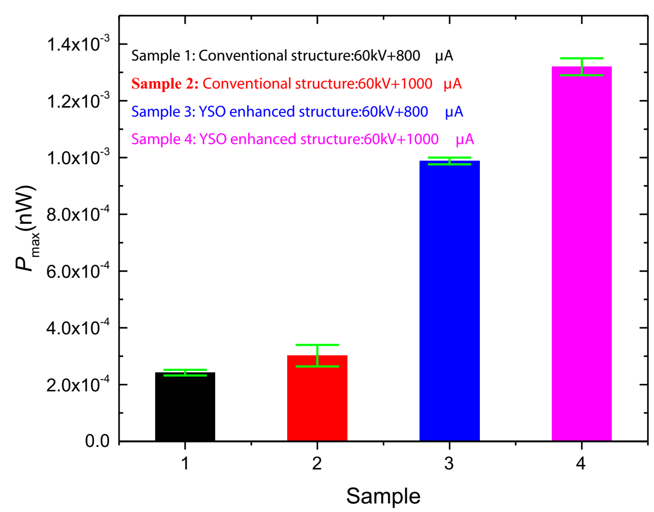

Fig. 12. Maximum output power comparison chart for both battery structures under different X-ray excitation conditions.

400 μA; (4) tube voltage: 52 kV, tube current: 800 μA: (5) tube voltage: 60 kV, tube current: 800 μA: (6) tube voltage: 60 kV, tube current: 1000 μA. The radiation resistance of the YSO crystal was evaluated by observing the changes in *FF* with time. The relationship between the changes in *FF* and the time is shown in Fig. 13.

Fig. 13 shows that there was no obvious variation in *FF* over time under the same excitation conditions. The values of *FF* were stabilised at approximately 0.31, 0.35, 0.50, 0.55, 0.57 and 0.59 under the six different excitation conditions, respectively. From

Table 4
Comparison of short-circuit current, open-circuit voltage, maximum output power and efficiency (Models A and B).

Battery structure	Excitation conditions	I_{sc} (nA)	V_{oc} (mV)	P_{max} (nW)	η (%)
Model A	60 kV, 800 μA	0.202	4.27	2.42×10^{-4}	0.48
	60 kV, 1000 μA	0.269	4.96	3.02×10^{-4}	0.53
Model B	60 kV, 800 μA	0.535	7.00	9.88×10^{-4}	1.98
	60 kV, 1000 μA	0.746	9.01	13.2×10^{-4}	2.31

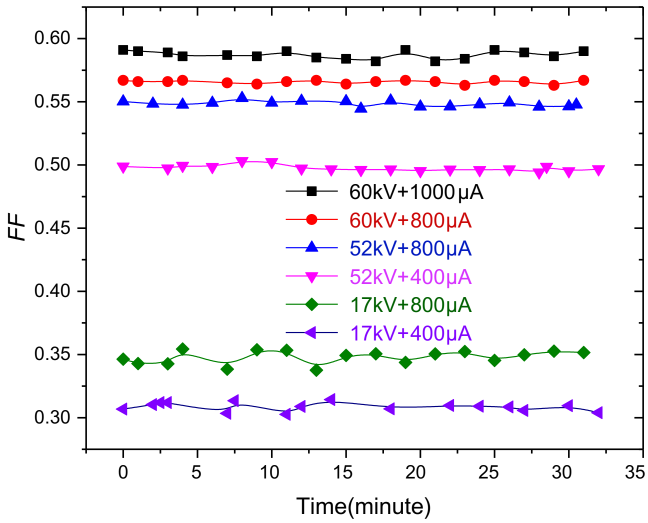

Fig. 13. Relationship between *FF* and time at different tube voltages and tube currents.

this result, it can be said that the performance of the YSO crystal did not significantly change after irradiation, and the crystal exhibited a high resistance to gamma irradiation for 30 min. In addition, the values of *FF* increased with an increase in the tube voltage and tube current.

4. Conclusions

A GaAs radiovoltaic cell enhanced by an YSO crystal was demonstrated for the first time using an X-ray tube to simulate the gamma rays emitted by a gamma-radioactive source. The electrical properties and the optical performance of this cell and the irradiation resistance of its YSO crystal were studied. Experimental results showed that there was a good match between the radioluminescence spectra of the YSO crystal and the spectral response curves of the GaAs device. Under both excitation conditions (tube voltage: 60 kV, tube current: 800 μA; tube voltage: 60 kV, tube current: 1000 μA), the values of I_{sc}, V_{oc} and P_{max} of the YSO crystal-enhanced structure were much greater than those of the conventional structure, especially in the case of P_{max}, which was more than quadruple that of the conventional structure. This clearly shows that the YSO crystal could significantly improve the output power and current of the cell. Under six different excitation conditions, the values of *FF* could be stabilised at approximately 0.31, 0.35, 0.50, 0.55, 0.57 and 0.59 in 30 min. This indicates that the YSO crystal has a high resistance to gamma irradiation that was developed quickly. In addition, it was found from the experimental results that the values of *FF* increased with an increase in the tube voltage and tube current.

Most of the X-ray energy cannot penetrate through the back electrode because of the tube voltage being no more than 60 kV, as provided by the existing X-ray tube in the laboratory, and only a small percentage of the X-ray energy can be absorbed by GaAs PV materials or the YSO crystal. This was the reason for the very low output power of both structures (conventional and YSO crystal-enhanced) in these experiments.

Acknowledgements

This work was supported by the National Natural Science Foundation of China (Grant Nos. 11675076 and 11505096), the Funding of Jiangsu Innovation Program for Graduate Education (Grant No. KYLX16_0354), the National Defense Basic Scientific Research Project (Grant No. JCKY2016605C006) and the Priority Academic Program Development of Jiangsu Higher Education Institutions.

References

[1] X. Lee, C. Wang, Optical design for uniform scanning in MEMS-based 3D imaging lidar, Appl. Opt. 54 (9) (2015) 2219–2223.
[2] J.H. Park, G.K. Garipov, J.A. Jeon, et al., Obscura telescope with a MEMS micromirror array for space observation of transient luminous phenomena or fast-moving objects, Opt. Express 16 (25) (2008) 20249–20257.
[3] M. Birkholz, K.E. Ehwald, T. Basmer, et al., Sensing glucose concentrations at GHz frequencies with a fully embedded Biomicro-electromechanical system (BioMEMS), J. Appl. Phys. 113 (24) (2013) 244904.
[4] L. Hong, X.B. Tang, Z.H. Xu, Y.P. Liu, D. Chen, Radioluminescent nuclear batteries with different phosphor layers, Nucl. Instrum. Methods Phys. Res. B 338 (2014) 112–118.
[5] D.Y. Qiao, X.J. Chen, Y. Ren, et al., A micro nuclear battery based on sic schottky barrierdiode, J. Microelectromech. Syst. 20 (3) (2011) 685–690.
[6] S.Z. Luo, G.Q. Wang, H.M. Zhang, Advance in radiovoltaic isotope battery, J. Isot. 24 (1) (2011) 002.
[7] A. Sharma, J. Melancon, S. Bailey, et al., Novel use of semiconductive conjugated polymer with optimized scintillator for betavoltaic applications, ASME V06BT07A041 (2015).
[8] C. Thomas, S. Portnoff, M.G. Spencer, High efficiency 4H-SiC betavoltaic power sources using tritium radioisotopes, Appl. Phys. Lett. 108 (1) (2016) 013505.
[9] D.Y. Qiao, X.J. Chen, Y. Ren, et al., A nuclear micro-battery based on silicon PIN diode, Acta Physica Sinica 60 (2) (2011) 020701.
[10] S. Butera, G. Lioliou, A.M. Barnett, Gallium arsenide ^{55}Fe X-ray-photovoltaic battery, J. Appl. Phys. 119 (6) (2016) 064504.
[11] S. Butera, G. Lioliou, A.B. Krysa, et al., $Al_{0.52}In_{0.48}P$ ^{55}Fe x-ray-photovoltaic battery, J. Phys. D Appl. Phys. 49 (35) (2016) 355601.
[12] L.C. Olsen, P. Cabauy, B.J. Elkind, Betavoltaic power sources, Phys. Today 65 (12) (2012) 35–38.
[13] H. Li, Y. Liu, R. Hu, et al., Simulations about self-absorption of tritium in titanium tritide and the energy deposition in a silicon Schottky barrier diode, Appl. Radiat. Isot. 70 (11) (2012) 2559–2563.
[14] G.A. Landis, S.G. Bailey, E.B. Clark, et al., Non-solar photovoltaics for small space missions, Photovoltaic Specialists Conference IEEE 42 (2012) 002819–002824.
[15] C. Delfaure, M. Pomorski, J. De Sanoit, et al., Single crystal CVD diamond membranes for betavoltaic cells, Appl. Phys. Lett. 108 (25) (2016) 252105.
[16] S. Tarelkin, V. Bormashov, E. Korostylev, et al., Comparative study of different metals for Schottky barrier diamond betavoltaic power converter by EBIC technique, Physica Status Solidi A (2016).
[17] H. Wang, X.B. Tang, Y.P. Liu, et al., Temperature effect on betavoltaic microbatteries based on Si and GaAs under ^{63}Ni and ^{147}Pm irradiation, Nucl. Instrum. Methods Phys. Res. B 359 (2015) 36–43.
[18] S.M. Sze, K.K. Ng, Physics of Semiconductor Devices, John Wiley & Sons, 2006.
[19] W.J. Choyke, G. Pensl, Physical properties of SiC, MRS Bull. 22 (03) (1997) 25–29.
[20] G. Lioliou, M.C. Mazzillo, A. Sciuto, et al., Electrical and ultraviolet characterization of 4H-SiC Schottky photodiodes, Opt. Express 23 (17) (2015) 21657–21670.
[21] G. Lioliou, X. Meng, J.S. Ng, et al., Temperature dependent characterization of gallium arsenide X-ray mesa pin photodiodes, J. Appl. Phys. 119 (12) (2016) 124507.
[22] E. Monroy, F. Omnès, F. Calle, Wide-bandgap semiconductor ultraviolet photodetectors, Semicond. Sci. Technol. 18 (4) (2003) R33.
[23] C.W. Thiel, W.R. Babbitt, R.L. Cone, Optical decoherence studies of yttrium oxyorthosilicate Y_2SiO_5 codoped with Er^{3+} and Eu^{3+} for optical signal processing and quantum information applications at 1.5 microns, Phys. Rev. B 85 (17) (2012) 174302.
[24] M. Nilsson, L. Rippe, N. Ohlsson, et al., Initial experiments concerning quantum information processing in rare-earth-ion doped crystals, Phys. Scr. 2002 (T102) (2002) 178–185.
[25] H.M. O'Bryan, P.K. Gallagher, G.W. Berkstresser, Thermal expansion of Y_2SiO_5 single crystals, J. Am. Ceram. Soc. 71 (1) (1988) C42–C43.
[26] J. Liang, A. Navrotsky, T. Ludwig, et al., Enthalpy of formation of rare-earth silicates Y_2SiO_5 and Yb_2SiO_5 and N-containing silicate $Y_{10}(SiO_4)_6N_2$, J. Mater. Res. 14 (4) (1999) 1181–1185.
[27] X.D. Wang, X.D. Xu, Z.W. Zhao, et al., Growth and spectral properties of Tm: Y_2SiO_5 single crystal, Acta Phys. Sin. 57 (8) (2008) 5007–5014.
[28] B. Liu, J. Wang, F. Li, et al., Mechanisms of mono-vacancy and oxygen permeability in Y_2SiO_5 orthosilicate studied by first-principles calculations, J. Am. Ceram. Soc. 95 (3) (2012) 1093–1099.
[29] Z. Sun, M. Li, Y. Zhou, Thermal properties of single-phase Y_2SiO_5, J. Eur. Ceram. Soc. 29 (4) (2009) 551–557.
[30] B. Xu, L. Cao, J. Huang, et al., Synthesis of yttrium silicates nanocrystallites by microwave-hydrothermal method, J. Synth. Cryst. 38 (6) (2009) 1329–1332.